INTRAMOLECULARLY HYPERCOORDINATED ORGANOLEAD COMPOUNDS: (o-$MeOC_6H_4$-CH_2)$PbPh_2R$, R = Ph, Cl, WITH Pb--O SECONDARY BONDING

Hemant K. Sharma [1], Alejandro J. Metta-Magaña [1], Laura I. Saucedo [1], Marcela López-Cardoso[2] and Keith H. Pannell[1*]

[1]Department of Chemistry and Biochemistry, The University of Texas at El Paso, El Paso, TX 79968

[2]Centro de Ciencias Químicas, Universidad Autónoma del Estado de Morelos, Cuernavaca, Morelos, MX

**Corresponding author; Email: kpannell@utep.edu*

Abstract.–The tetrahedral geometry of organolead(IV) compounds can be readily transformed by using an organic ligand containing a dangling-arm oxygen functionality. The acidity of the Pb center results in so-called secondary bonding between O and Pb thereby pushing the geometry at Pb toward a trigonal bipyramidal (tbp) structure. Replacing a phenyl group by a chlorine atom dramatically enhances this phenomenon. Thus for (o-methoxybenzyl) triphenyllead (**4**), and (o-methoxybenzyl)diphenyllead chloride (**5**), the Pb--O internuclear distances are 3.362(4) and 2.845(3) Å, respectively; 83% (**4**) and 70% (**5**) of the sum of the van der Waals Pb and O radii. Within the group 14 element congeners the structural analysis of the (o-methoxybenzyl)triphenylE compounds, E = Si, Ge, Sn, and now Pb, demonstrates the relative acidities of E are Si < Ge < Sn < Pb.

Keywords: hypercoordination, dangling-arm ligands, oxygen secondary bonding, group 14 Lewis acidity

---

Since the structural analysis of the pyridine adduct of trimethyltinchloride, $PyMe_3SnCl$ (Hulme 1963), there has been a consistent interest in the so-called hypercoordinated compounds of the heavy group 14 elements, where 5 and 6 coordinate materials exhibit interesting structural and chemical variations compared to the normal tetrahedral arrangement of these elements in their tetravalent state (Khan & Foucher 2016). In the case of silicon, the interest of early researchers (Chuit et al. 1993; Bassindale et al. 2003; 2010) was focused upon the study of proposed intermediates in the mechanism of displacement reactions at the silicon center. In the more studied case of tin, the search for entertaining structural motifs (Colton &

OPEN ACCESS DOI 10.32011/txjsci_73_1_Article2
Received: 20 May 2020 | Accepted: 21 December 2020 | Published Online: 11 January 2021

Dakternieks 1988), potential biological activity (Li et al. 1996; Lébl et al. 2003; Raychaudhury et al. 2005; Vargas et al. 2017), and interesting new organotin polymers and oligomers (Khan et al. 2015), are all stimulants for this research activity.

Related studies on germanium and lead are less prevalent and indeed the study of organolead chemistry in general has become a quiet backwater within the general area of organometallic chemistry. Although a check on "organolead" in the current literature will result in many very interesting recent studies, they are focused upon lead perovskite salts, where the organo-ammonium cation reveals the reason for "organo"; however, no lead-carbon bond interactions are present (Cai et al. 2013). Reports on intramolecularly hypercoordinated Pb compounds are very limited. An early such interaction was reported for $(Me_2NCH_2CH_2CH_2)Ph_2PbI$, with a Pb--N internuclear distance of 2.677 Å (Figure 1A) (Zickgraf et al. 1998). A later report described the synthesis and structure of the related (o-Me_2NCH_2-C_6H_4)$Ph_2Pb(Cl)$ with a Pb--N internuclear distance of 2.64(18) Å (Figure 1B) (Cristea et al. 2009). In both examples the intramolecular Pb--N interaction is *trans* axial to the halogen atom in a structure transitioning to trigonal bipyramidal (tbp).

We have a longstanding interest in intramolecular hypercoordination within the group 14 elements and have reported on the variations of intramolecular interactions for the (o-methylthiobenzyl)triphenyl-element system, (o-$MeSC_6H_4CH_2$)EPh_3, E = Si, Ge, Sn, Pb, Figure 2A, involving potential, and discovered, E--S

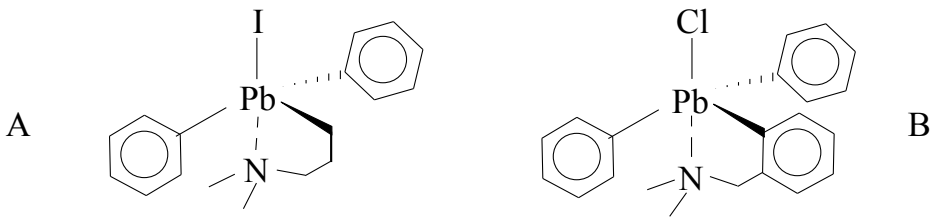

Figure 1. Structurally characterized intramolecularly hypercoordinate organolead compounds.

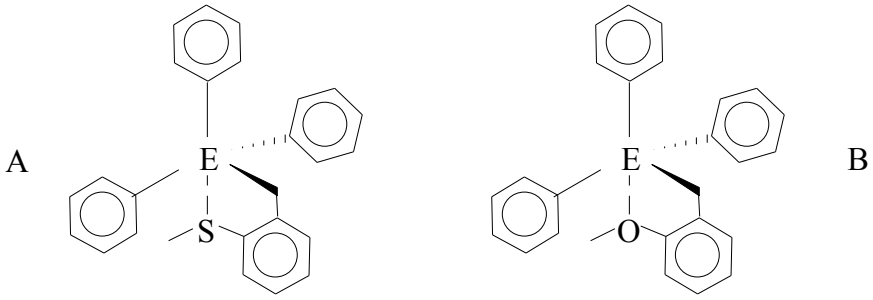

Figure 2. (o-$MeSC_6H_4CH_2$)EPh_3, E = Si, Ge, Sn, Pb (A); (o-$MeOC_6H_4CH_2$)EPh_3, E = Si (**1**), Ge (**2**) , Sn (**3**) , Pb (**4**) (B).

interactions (Munguia et al. 2003). From this study it was clear that for the tetraorganometallics ($E(C)_4$) the Lewis acidity of the central element was restricted to Sn and Pb, as might be expected due to the significantly more metallic character of these heavy elements. More recently a synthetic, structural, and DFT study of the related oxygen triphenylbenzyl derivatives (o-$MeOC_6H_4CH_2$)EPh_3, E = Si (**1**), Ge (**2**), Sn (**3**), Pb (**4**) (Figure 2B) detailed the extent of any intramolecular E--O interactions (López-Cardoso et al. 2018).

For the E = Si and Ge compounds, **1** and **2**, both the experimental structural analysis and computational calculations resulted in no significant intramolecular interaction between E and the dangling arm O atom. The internuclear E--O distance was well above the sum of the van der Waals radii for E and O (Chauvin 1992), and the geometries at the central element E, were effectively tetrahedral, 98% (**1**); 96.5% (**2**). We had previously published the structure of the tin compound **3** and observed a distinct deviation of the geometry at Sn toward a trigonal bipyramidal structure and noted a Sn--O intermolecular distance of 3.074 Å, which represented 79% of the sum of the Sn and O VdW radii (Munguia et al 2007). Clearly the tin atom was, as predicted by the DFT calculations, considerably more acidic than both Si and Ge in the series **1**, **2**, **3**, and **4**.

Unfortunately, at the time of that article the lead compound, (o-$MeOC_6H_4CH_2$)$PbPh_3$ (**4**), was not available in crystalline form;

however, the DFT calculation predicted a significant Pb--O interaction of 3.45 Å and a distortion from a tetrahedral structure at the Pb atom due to that intramolecular interaction.

We now report the structure of **4**, and that of the related compound (o-$MeOC_6H_4CH_2$)$PbPh_2Cl$, **5**, where the replacement of a phenyl group by chlorine atom will be expected to dramatically enhance any Lewis acidity of the lead atom and thereby augment any intramolecular Pb--O interaction.

MATERIALS AND METHODS

Experimental: Synthesis of o-methoxybenzylchlorodiphenyllead. – A 10 mL screw capped vial equipped with a small magnetic stir bar was charged with 0.14 g (0.25 mmol) of *o*-methoxybenzyltriphenyllead, **4** (López-Cardoso et al. 2018), in 2 mL of $CDCl_3$. To the vial, maintained at -25 ^oC, was added dropwise *via* a micro syringe 0.25 mL of (1.0 M) HCl solution in ether. The reaction was maintained at low temperature for 30 min. ^{207}Pb NMR spectroscopic monitoring showed that the initial resonance of **4** at -152.1 ppm disappeared and was replaced by a new resonance at 83.8 ppm due to the formation of (o-$MeOC_6H_4$-CH_2)$PbPh_2Cl$. The white crystalline solid 0.085 g (66 % yield) was recrystallized from hexane/$CDCl_3$ mixture. ^{1}HNMR ($CDCl_3$): 3.61(s, 3H, O-Me), 3.74 (s, 2H, CH_2), 6.70-7.51 (complex multiplets, 14H, Ph); ^{13}CNMR: 40.2 (CH_2), 55.1 (O-Me), 109.5, 121.3,127.0, 127.8, 129.4. 129.9, 130.2, 125.8, 155.5, 159.2 (Ph); ^{207}Pb: 83.8 ppm.

Structural analysis.–The X-ray intensity data of compound **4** was measured on a Photon 200 Bruker D8 VENTURE Duo system equipped with a microfocus (MoKα, λ = 0.71073 Å) and a HELIOS multilayer optics monochromator. The X-ray intensity data of compound **5** were measured on a Bruker SMART APEX CCD system equipped with a fine-focus tube (MoKα, λ = 0.71073 Å) and a

graphite monochromator. In both cases, the frames were integrated with the Bruker SAINT software package using a narrow-frame algorithm. In addition, it was corrected for absorption effects using the multi-scan method (SADABS). The structure was solved with the intrinsic phasing method and refined using the Bruker SHELXTL Software Package.

RESULTS AND DISCUSSION

The synthesis and characterization of **4** was as previously described (López-Cardoso et al. 2018) involving the *in-situ* reaction between o-methoxybenzyl chloride and Ph_3PbCl in the presence of an excess of magnesium turnings, Equation 1. The ^{1}H and ^{13}C NMR characterization of the material was as reported, with the exception that our ^{207}Pb NMR exhibited a single resonance at -152.1 ppm, rather than that reported at -181 ppm. Compound **4** crystallized in space group $P2_1/c$ and the ORTEP structural representation is illustrated in Figure 3 and selected crystallographic data are reported in Table 1.

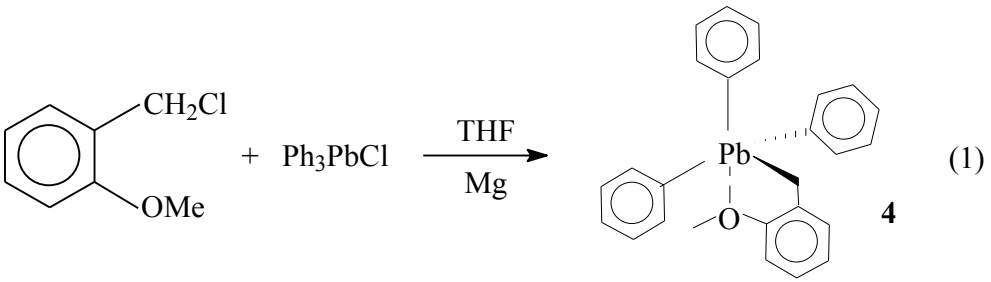

Compound **4** has a single conformer in the asymmetric unit cell with a Pb--O distance of 3.362(4) Å. As noted above, the DFT calculations (using the basis set LACVP) on **4** predicted an intramolecular Pb--O interaction of 3.45 Å. This longer than experimental internuclear distance was typical of the other calculated

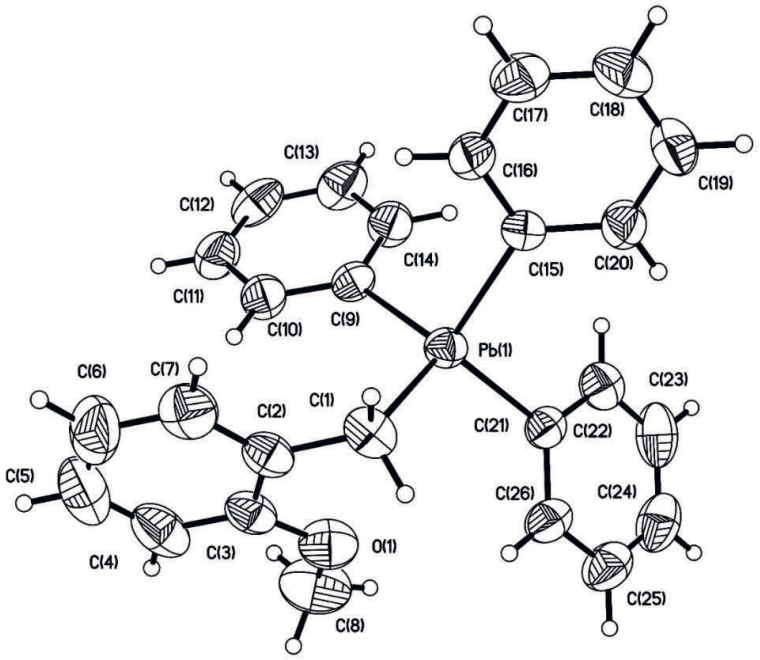

Figure 3. ORTEP structural representation of **4**; Pb--O internuclear distance is 3.362(4) Å.

Table 1 Selected crystallographic data for **4** and **5**. CCDC 2003827 and 2003826 contain the supplementary data of **4** and **5** respectively and can be accessed from the Cambridge Crystallographic Data Centre via www.ccdc.cam.ac.uk/structures.

	4	**5**
Chemical formula	$C_{26}H_{24}OPb$	$C_{20}H_{19}ClOPb$
Formula weight	559.64 g/mol	517.99 g/mol
Temperature	299(2) K	296(2) K
Crystal system	monoclinic	monoclinic
Space group	P 1 21/c 1	P 1 21/c 1
a (Å)	16.9746(7)	8.4428(11)
b (Å)	19.4377(7)	26.555(4)
c (Å)	6.8107(3)	8.8485(12)
α (°)	90	90
β (°)	97.490(2)	109.182(2)
γ (°)	90	90
Volume ($Å^3$)	2228.00(16)	1873.7(4)
R_1 all data	0.0907	0.0485
R_1 I>2σ(I)	0.0400	0.0310

vs experimental values for all the group 14 series of compounds, and probably reflects the current inadequacy of the basis sets used for the heavy element materials and possible crystal packing forces. However, the result is that compound **4** does exhibit a significant intramolecular hypercoodination as predicted. Furthermore, the geometry at the Pb atom exhibits an experimental value of 74% Td structure, *vide infra* Table 3 and further discussion, illustrating the strength of the intramolecular Pb--O interaction even in this tetraorganolead material.

The transformation of **4** to the mono-chloro derivative (o-$MeOC_6H_4CH_2$)$PbPh_2Cl$ (**5**) was readily accomplished in good yield by treatment of **4** with one equivalent of an HCl/Et_2O solution, Equation 2.

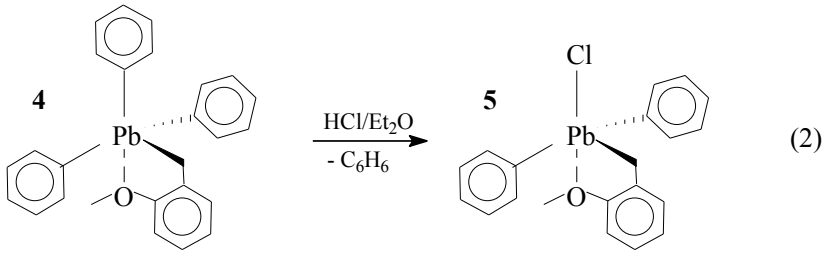

(2)

The ^{1}H, ^{13}C and ^{207}Pb NMR data for **5** are in accord with the formulation. In particular the ^{207}Pb NMR chemical shift of 83.8 ppm exhibits the change expected for the transformation of the tetraorganolead **4** (with limited hypercoordination) to a triorganolead chloride with significant hypercoordination (Margolis et al. 2003). These NMR trends are similar to those well-established by ^{119}Sn NMR studies on related materials (Holaćek et al. 1983; Colton & Dakternieks 1988; Munguia et al. 2007).

The ORTEP representation of the structure of **5**, also with a single conformer in the unit cell, is illustrated in Figure 4 and exhibits a much closer Pb--O internuclear distance of 2.845 Å, compared to **4** at 3.362 Å, and a significantly lower Td structure (31%, Table 2), i.e. it is much closer to a tbp geometry.

In Table 2 we summarize the pertinent structural data for **4** and **5**, along with the data for **1**, **2** and **3** for ready comparison. The estimates of Td geometries involve comparing the sum of the equatorial angles for tetrahedral and trigonal bipyramidal, 328.5 and 360° respectively, to the observed values. The resulting data are in accord with the increasing Lewis acidity of the central element and intramolecular E--O interactions; the replacement of Ph group in **4** by Cl in **5** is dramatic.

We performed DFT calculations using the LanL2DZ basis set from the Gaussian 09 system (Frisch et al. 2010), which has been suggested for heavy elements such as Pb (Wadt & Hay 1985; Lyczko 2017). These computations, Table 3, predicted an intramolecular Pb--O distance in **4** of 3.54 Å, and 2.69 Å for **5**, somewhat less accurate than the LACVP basis set used by López-Cardoso et al. The data do however predict the significantly reduced Pb--O internuclear distance upon substituting a Ph group of **4** by a chlorine in **5**. The other geometrical aspects of the two molecules **4** and **5** are reasonably in agreement with the experimental data in terms of bond lengths and angles, and also illustrate the reduced percentage of Td structure from **4** (91%) to **5** (36%) using the Eq method.

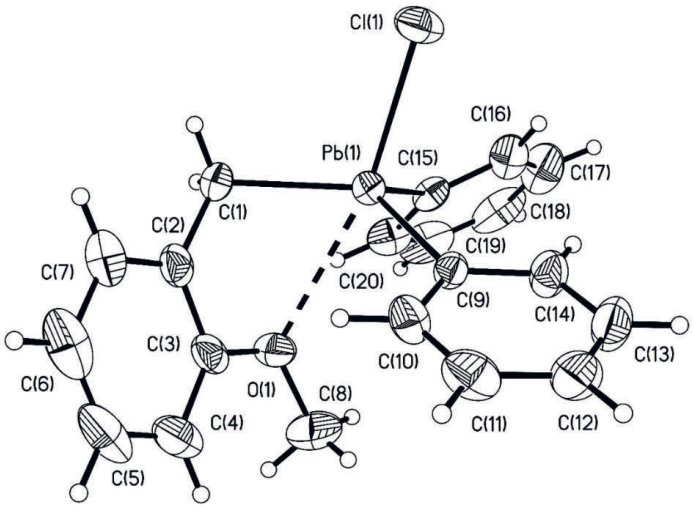

Figure 4. ORTEP representation of the structure of **5**; Pb--O internuclear distance is 2.845(3) Å.

Table 2. Contacts and tetrahedral character values compounds **1** – **5**.

	M--O	ΣVdW (Å)	Contact (Å)	%VdW	% Td Eq method
1	Si--O	3.61	3.810	106	97.7
2	Ge--O	3.66	3.802	104	95.9
3	Sn--O	3.91	3.074	79	84.3
4	Pb--O	4.04	3.362	83	73.6
5	Pb--O	4.04	2.845	71	30.7

Overall, these results confirm the gradually increasing acidity of the elements in the order Si < Ge < Sn <Pb with respect to both O (this work) and S (Munguia et al. 2003) dangling arm ligands in homologous systems. Both the decreasing Pb--O internuclear distances and the increasing tbp geometry at Pb arrive at the same conclusion. The synthesis, and structural/spectroscopic analysis, of the new organolead compound **5** further confirms the tendency for increasingly electronegative groups at the central Pb center to augment the Lewis acidity of that group 14 metal.

Table 3. Selected bond lengths (Å) and angles (°) for **4** and **5** compared to selected data computed using LANL2DZ. The bulk of computed data is available from the authors.

Compound **4**			Compound **5**		
	Crystal	LanL2DZ		Crystal	LanL2DZ
Pb1-O1	3.362(4)	3.54	Pb1-O1	2.845(3)	2.69
Pb1-C1	2.235(5)	2.22	Pb1-Cl	2.218(4)	2.20
Pb1-C9	2.222(4)	2.18	Pb1-C9	2.209(4)	
Pb1-C15	2.210(4)		Pb1-C15	2.211(4)	
Pb1-C21	2.215(4)		Pb1-Cl1	2.5215(11)	2.53
O1-C3	1.367(7)		O1-C3	1.377(5)	
O1-C8	1.421(7)		O1-C8	1.426(6)	
C3-O1-C8	117.6(5)		C3-O1-C8	118.5(4)	
C15-Pb-O1	158.9(1)	140.64	Cl1-Pb1-O1	166.49(8)	165.98
Equatorial			Equatorial		
C1-Pb1-C9	113.66(17)	112.90	C1-Pb1-C9	120.59(14)	119.19
C1-Pb1-C21	113.65(19)	110.84	C1-Pb1-C15	118.29(15)	118.17
C9-Pb1-C21	109.52(15)	107.73	C9-Pb1-C15	111.44(14)	111.34
Axial			Axial		
C15-Pb1-C1	106.17(16)	107.04	Cl1-Pb1-C1	103.60(11)	99.87
C15-Pb1-C9	105.57(15)	108.72	Cl1-Pb1-C9	97.86(9)	100.63
C15-Pb1-C21	107.72(15)	109.57	Cl1-Pb1-C15	99.62(11)	103.57

ACKNOWLEDGMENTS

We are thankful for support by the Welch Foundation (Grant AH-0546), the Kresge Foundation for upkeep of our NMR facility, and the NSF MRI program (CHE-1827875 for purchase the VENTURE system.

LITERATURE CITED

Bassindale, A. R., D. J. Parker, P. G. Taylor, N. Auner & B. Herrschaft. 2003. Modeling S_N2 nucleophilic substitution at silicon by structural correlation with X-ray crystallography and NMR spectroscopy. Organomet. Chem. 667:66-72.

Bassindale A. R., M. Sohail, P. G. Taylor, A. A. Korlyukov & D. E. Arkhipov. 2010. Four independent structures of a pentacoordinate silicon species at different points on the Berry pseudorotation pathway. Chem. Commun. (Cambridge, England), 46:3274-3276.

Cai, B., Y. Xing, Z. Yang, W-H. Zhang & J. Qiu. 2013. High performance hybrid solar cells sensitized by organolead halides perovskites. Energy Environ. Sci. 6:1480-1485.

Chauvin, R. 1992. Explicit periodic trend of van der Walls radii. 96:9194-9197.

Chuit, C., R. J. P. Corriu, C. Reye & J. C. Young. 1993. Reactivity of penta- and hexacoordinate silicon compounds and their role as reaction intermediates. Chem. Rev. 93:1371-1448.

Colton, R., & D. Dakternieks. 1988. Tin-119 NMR studies on diorganotin(IV)dihalides and triorganotin(IV)halides: Formation and stereochemistry of adducts. Inorg. Chim. Acta 148:31-36.

Cristea, A., A. Silvestru & C. Silvestru. 2009. Hypervalent tetra- and triorganolead(IV) compounds containing 2-$(R_2NCH_2)C_6H_4$ groups (R = Me, Et). Studia Universitatis Babes-Bolyai. Chemia, 4:223-235.

Frisch, M. J., G. W. Trucks, H. B. Schlegel, G. E. Scuseria, M. A. Robb, J. R. Cheeseman, G. Scalmani, V. Barone, B. Mennucci, G. A. Petersson, H. Nakatsuji, M. Caricato, X. Li, H. P. Hratchian, A. F. Izmaylov, J. Bloino, G. Zheng, J. L. Sonnenberg, M. Hada, M. Ehara, K. Toyota, R. Fukuda, J. Hasegawa, M. Ishida, T. Nakajima, Y. Honda, O. Kitao, H. Nakai, T. Vreven, J. A. Montgomery, Jr., J. E. Peralta, F. Ogliaro, M. Bearpark, J. J. Heyd, E. Brothers, K. N. Kudin, V. N. Staroverov, T. Keith, R. Kobayashi, J. Normand, K. Raghavachari, A. Rendell, J. C. Burant, S. S. Iyengar, J. Tomasi, M. Cossi, N. Rega, J. M. Millam, M. Klene, J. E. Knox, J. B. Cross, V. Bakken, C. Adamo, J. Jaramillo, R. Gomperts, R. E. Stratmann, O. Yazyev, A. J. Austin, R. Cammi, C. Pomelli, J. W. Ochterski, R. L. Martin, K. Morokuma, V. G. Zakrzewski, G. A. Voth, P. Salvador, J. J. Dannenberg, S. Dapprich, A. D. Daniels, O. Farkas, J. B. Foresman, J. V. Ortiz, J. Cioslowski & D. J. Fox. 2010. Gaussian 09, Revision C.01, Gaussian, Inc., Wallingford CT.

Holaćek, J., M. Nadvornik, K. Handlir & A. Lyćka. 1983. ^{13}C and ^{119}Sn NMR study of some four and five-coordinate triphenyltin(IV) compounds. J. Organomet. Chem. 241:177-184.

Hulme, R. 1963. The crystal and molecular structure of chloro(trimethyl)pyridinetin(IV). J. Chem. Soc. 1524-1527.

Khan, A. & D. Foucher. 2016. Hypercoordinate compounds of the group 14 elements containing κ^n-C,N-, C,O-, C,S- and C,P-ligands. Coord. Chem. Rev. 312:41-66.

Khan, A, S. Komejan, A. Patel, C. Lombardi, A. J. Lough & D. A. Foucher. 2015. Reduction of C,O-chelated organotin(IV) dichlorides and dihydrides leading to protected polystannanes. J. Organomet. Chem. 776:180-191

Lébl, T., A. Smicka, J. Brus & C. Bruhn. 2003. Synthesis, structural study, and in vitro trypanocidal and antitumour activities of tetrakis(3-methoxypropyl)tin and (3-methoxypropyl)tin chlorides. Eur. J. Inorg. Chem. 143-148.

Li, Q., P. Yang, E. Hau & C. Tian. 1996. Diorganotin(IV) antitumor agents. Aqueous and solid-state coordination chemistry of nucleotides with R_2SnCl_2. J. Coord. Chem. 40:227-236.

López-Cardoso, M., G. Vargas-Pineda, P. Román-Bravo, M. E. Rosas-Valdez, A. Ariza-Roldan, R. S. Razo-Hernández, K. Pannell & R. Cea-Olivares. 2018. Synthesis, structural investigation and DFT studies on the intramolecular interaction in group 14 (2-$CH_3OC_6H_4CH_2$)MPh_3, M = Si, Ge, Sn, Pb) organometallic compounds. Inorg. Chim. Acta, 475:28-34.

Lyczko, K. 2017. Tropolone as anionic and neutral ligand in lead (II) and Bi (III) complexes: Synthesis, structural characterization and computational studies. J. Mol. Struct. 1127:549-556.

Margolis, L. A., C. D. Schaeffer Jr., & C. H. Yoder. 2003. A ^{207}Pb NMR study of the adducts of triphenyllead chloride and diphenyllead dichloride. Appl. Organomet. Chem. 17:236-238.

Munguia, T., I. S. Pavel, R. N. Kapoor, F. Cervantes-Lee, L. Párkányi & K. H. Pannell. 2003. Lewis acidity of group 14 elements toward intramolecular sulfur in ortho-aryl-thioanisoles. Can. J. Chem. 81:1388-1397.

Munguia, T., M. López-Cardoso, F. Cervantes-Lee & K. H. Pannell. 2007. Intramolecular chalcogen-tin interactions in (o-$MeEC_6H_4CH_2$)$SnPh_{3-n}Cl_n$ (E = S, O; n = 0, 1, 2), characterized by Xray diffraction and ^{119}Sn solution and solid state NMR. Inorg. Chem. 46:1305-1313.

Raychaudhury, B., S. Banerjee, S. Gupta, R. V. Singh & S. C. Datta. 2005. Antiparasitic activity of a triphenyl tin complex against *Leishmania donovani.* Acta Tropica, 95:1-8.

Vargas, D. G., A. Metta-Magaña, H. K. Sharma, M. M. Whalen, T. M. Gilbert & K. H. Pannell. 2017. A potential "green" organotin: Bis-(methylthiopropyl)tin dichloride. Inorg. Chim. Acta, 468:125-130.

Wadt, W. R. & P. J. Hay. 1985. Ab initio effective core potentials for molecular calculations. Potentials for main group elements Na to Bi. J. Chem. Phys. 82:284-298

Zickgraf, A., M. Beuter, U. Kolb, M. Drager, R. Tozer, D. Dakternieks & K. Jurkschat. 1998. Nucleophilic attack within Ge, Sn and Pb complexes containing $Me_2N(CH_2)_3$ as a potential intramolecular donor ligand. Inorg. Chim. Acta, 275-276:203-214.